

Internal dosimetry as a tool for radiation protection of the patient in nuclear medicine

MG Stabin^{*,1}, PhD, CHP, GD Flux², PhD

¹ Vanderbilt University, Nashville, Tennessee, United States

² Department of Physics, Royal Marsden Hospital, London, United Kingdom

Received 12 January 2007; accepted 24 January 2007

INTRODUCTION

A number of radioactive therapeutic agents are currently employed against various forms of cancer and other diseases. In radiotherapy with external sources of radiation (including brachytherapy), patient-individualised dose calculations are always performed prior to therapy and form an essential basis of the patient treatment plan. Patient-individualised dose calculations, however, are usually not calculated to optimise this process in the therapeutic use of radiopharmaceuticals. This article reviews the current status of dose calculations for radiopharmaceuticals and discusses the need for patient-individualised dose calculations to optimise therapy for patients and provide improved clinical outcomes.

STANDARDISED METHODS AND MODELS FOR INTERNAL DOSE CALCULATIONS

Reliable estimates of radiation-absorbed dose from the use of diagnostic or therapeutic radiopharmaceuticals in nuclear medicine are essential to the evaluation of the risks and benefits of their use. To estimate absorbed dose for all significant tissues, one must determine the

quantity for each tissue. The absorbed dose is defined as the amount of energy from ionising radiation that is absorbed per unit mass of any material. These authors' interest in the evaluation of dose from radiopharmaceuticals is in the energy deposited in human tissues.

Standard Dose equations

A generic equation for the absorbed dose rate in an object uniformly contaminated with radioactivity (for example an organ or tissue with radiopharmaceutical uptake) may be shown as:

$$\dot{D}_T = \frac{k A_S \sum_i y_i E_i \phi_i}{m_T} \quad (1)$$

where,

\dot{D}_T = absorbed dose rate to a target region of interest (Gy/sec or rad/hr)

A_S = activity (MBq or μ Ci) in source region S

y_i = number of radiations with energy E_i emitted per nuclear transition

E_i = energy per radiation for the i th radiation (MeV)

ϕ_i = fraction of energy emitted in a source region that is absorbed in a target region

m_T = mass of the target region (kg or g)

k = proportionality constant (Gy-kg/MBq-sec-MeV or rad-g/ μ Ci-hr-MeV)

* Corresponding author. Present address: Department of Radiology and Radiological Sciences, Vanderbilt University, 1161 21st Avenue South, Nashville, TN 37232-2675, United States. Tel.: (615) 343 0068; Fax: (615) 322 3764; E-mail: michael.g.stabin@vanderbilt.edu (Michael G. Stabin).

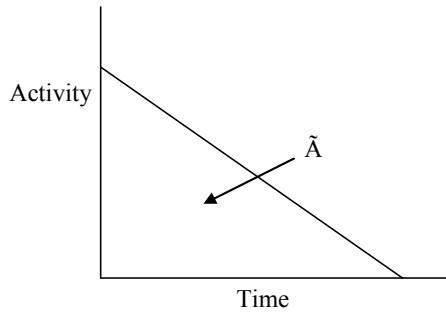


Figure 1 General time/activity curve for an internal emitter.

The proportionality constant k includes the various factors that are needed to obtain the dose rate in the desired units, from the units employed for the other variables, and it is essential that this factor is properly calculated and applied. For example, if the dose rate is wanted in rad/hr, and there are employed units of μCi for activity, MeV for energy and g for mass, the conversions that are needed are:

$$k = \frac{3.7 \times 10^4 \text{ dis}}{\text{sec} - \mu\text{Ci}} \frac{3600 \text{ sec}}{\text{hr}} \frac{\text{rad} - \text{g}}{100 \text{ erg}} \frac{1.6 \times 10^{-6} \text{ erg}}{1 \text{ MeV}} \quad (2)$$

$$= 2.13 \frac{\text{rad} - \text{g}}{\mu\text{Ci} - \text{hr} - \text{MeV}}$$

If instead the dose rate is wanted in Gy/sec, and there are employed units of MBq for activity, MeV for energy and kg for mass, the conversions needed are:

$$k = \frac{1 \text{ dis}}{\text{sec} - \text{MBq}} \frac{\text{Gy} - \text{kg}}{1 \text{ J}} \frac{1.6 \times 10^{-9} \text{ J}}{1 \text{ MeV}} \frac{1000 \text{ mGy}}{\text{Gy}} \quad (3)$$

$$= 1.6 \times 10^{-6} \frac{\text{mGy} - \text{kg}}{\text{MBq} - \text{sec} - \text{MeV}}$$

Often investigators require an estimate of *total absorbed dose*, rather than just the instantaneous dose rate at some point in time, from a radiopharmaceutical administration. In the dose equation, the quantity activity (nuclear transitions per unit time) causes the outcome of the equation to have time dependence. To calculate the cumulative dose, the time integral of the dose equation must be calculated. In most cases, the only term which depends on time is activity, so the only factor that has to be integrated is the activity term. The integral of the time-activity curve (i.e. the area under that curve, regardless of its shape), is often called the *cumulated activity* (often given the symbol \tilde{A}), and it represents the total number of disintegrations that have occurred over time in a source region.

Therefore, the equation for cumulative dose becomes:

$$D_T = \int \dot{D}_T dt = \frac{k \tilde{A}_S \sum_i y_i E_i \phi_i}{m_T} \quad (4)$$

where D is the absorbed dose (Gy or rad) and the quantity \tilde{A}_S represents the integral of $A_S(t)$, the time-dependent activity within the source region:

$$\tilde{A}_S = \int_0^\infty A_S(t) dt = A_0 \int_0^\infty f_S(t) dt \quad (5)$$

where A_0 is the activity administered to the patient at time $t = 0$, and $f_S(t)$ may be called the fractional distribution function for a source region (fraction of administered activity present within the source region at time t). In many instances, the function $f_S(t)$ may be modeled as a sum of exponential functions:

$$f_S(t) = f_1 e^{-(\lambda_1 + \lambda_p)t} + f_2 e^{-(\lambda_2 + \lambda_p)t} + \dots + f_N e^{-(\lambda_N + \lambda_p)t} \quad (6)$$

where terms $f_1 \dots f_N$ represent the fractional uptake of the administered activity within the 1st to Nth compartments of the source region, $\lambda_1 \dots \lambda_N$ represent the biological elimination constants for these same compartments, and λ_p represents the physical decay constant for the radionuclide of interest. Other functional expressions may be used to represent the fractional distribution function, but exponentials are most commonly encountered.

A generalised expression for calculating internal dose, which may describe the equations shown in publications by different authors, can be calculated by the following equation:

$$D = N \times DF \quad (7)$$

where N is the number of nuclear transitions that occur in source region S (identical to \tilde{A}_S), and DF is a ‘‘dose factor’’. The factor DF contains the various components shown in the formulas for S and SEE (and in some presentations may as well include a ‘radiation weighting factor’, w_R); it depends on combining decay data with absorbed fractions (AFs), which are derived generally using Monte Carlo simulation of radiation transport in models of the body and its internal structures (organs, tumours, etc.):

$$DF = \frac{k \sum_i y_i E_i \phi_i w_{R_i}}{m_T} \quad (8)$$

As written, the above equations give only the dose from one source region to one target region, but they can be generalised easily to multiple source regions:

$$D_T = \frac{k \sum_S \tilde{A}_S \sum_i y_i E_i \phi_i (T \leftarrow S) w_{R_i}}{m_T} \quad (9)$$

Available body models

The current generation of anthropomorphic phantoms began with the development of the Fisher-Snyder phantom [1], which employed a combination of geometric shapes - spheres, cylinders, cones, etc. - to create a reasonably accurate representation of the body. Monte Carlo computer programs were used to simulate the creation and transport of photons through these various structures in the body, whose atomic

compositions and densities were based on data provided by the International Commission on Radiological Protection (ICRP) in its widely quoted report on "Reference Man" [2], now updated in a more recent report [3]. These reports provide various anatomical data helpful in producing dose calculations for standardised individuals. Absorbed fractions and dose conversion factors (S values), as defined above, for over 100 radionuclides and over 20 source and target regions, were also published [4, 5].

Cristy and Eckerman [6] modified the adult male model and developed models for a series of individuals of different size and age. Six phantoms were developed, which were assumed to represent children of ages 0 (newborn), 1, 5, 10, and 15, and adults of both genders. Absorbed fractions for photons at discrete energies were published for these phantoms, which contained approximately 25 source and target regions. Tables of S values were never published, but ultimately were made available in the computer software called "MIRDOSE" [7], which was widely used by the nuclear medicine community. Stabin *et al.* developed a series of phantoms for the adult female, including a model of the non-pregnant adult female, and the woman at three stages of pregnancy.[8] These phantoms modeled the changes to the uterus, intestines, bladder, and other organs that occur during pregnancy, and included specific models for the fetus, fetal soft tissue, fetal skeleton, and placenta. S values for these phantoms were also made available to the dosimetry community through the MIRDOSE software[7].

Marrow dose models

Spiers *et al.* at the University of Leeds [9] first developed electron absorbed fractions (AFs) for bone and marrow for an adult male subject; these results were used to calculate dose conversion factors (DCFs), or S values, in MIRD Pamphlet No. 11 [5]. Eckerman [10] re-evaluated this work and extended the results to derive dose factors for 15 skeletal regions in six models representing individuals of various ages. The results were also used in the MIRDOSE 3 software [7] to provide average and regional marrow dose, and dose-volume histograms for individuals of different ages. Bouchet *et al.* [11] used newer information on regional bone and marrow mass, and calculated new AFs using the EGS4 Monte Carlo code. Although the results of the Eckerman and Bouchet *et al.* models were similar in most characteristics and reported results, the models differed in a few important underlying assumptions. A revised model, which resolves these model differences in ways best supported by currently available data, has been derived [12]. New skeletal average absorbed fractions for all bone regions employed in the calculations in this study were implemented in the OLINDA/EXM [13] computer code, designed as a successor to the MIRDOSE code [7].

Planar methods for quantification

In the introduction to MIRD Pamphlet No. 16 [14], the following is stated:

"To determine the activity-time profile of the radioactivity in source regions, four questions need to be answered:

1. What regions are source regions?
2. How fast does the radioactivity accumulate in these source regions?
3. How long does the activity remain in the source regions?
4. How much activity is in the source regions?

The first question concerns identification of the source regions while the second and third questions relate to the appropriate number of measurements to be made in the source regions as well as the timing of these measurements. The fourth question is addressed through quantitative external counting and/or sampling of tissues and excreta.

Each source region must be identified and its uptake and retention of activity as a function of time must be determined. This provides the data required to calculate cumulated activity or residence time in all source regions. Each region exhibiting significant radionuclide uptake should be evaluated directly where possible. The remainder of the body (total body minus the source regions) must usually be considered as a potential source as well. Mathematical models that describe the kinetic processes of a particular agent may be used to predict its behavior in regions where direct measurements are not possible, but where sufficient independent knowledge about the physiology of the region is available to specify its interrelationship with the regions or tissues whose uptake and retention can be measured directly. The statistical foundation of a data acquisition protocol designed for dosimetry requires an adequate number of data points and careful selection of the timing of these points. As the number of measurements increases, the confidence in the fit to the data and in the estimates of unknown parameters in the model is improved. As a heuristic or general rule of thumb, at least as many data points as the number of initially unknown variables in the mathematical curve-fitting function(s) or in the compartmental model applied to the data set, should be obtained. For example, each exponential term in a multiexponential curve-fitting function requires two data points to be adequately characterised. On the other hand, if it is known a priori that the activity retention in a region can be accurately represented by a monoexponential function, restrictions on sampling times are less stringent as long as enough data points are obtained to derive the fitted function. Because of problems inherent in the collection of patient data (e.g., patient motion, loss of specimen, etc), the collection of data above the necessary minimum is advisable."

The execution of a successful dosimetry study lies in the gathering of sufficient data to characterise the radiopharmaceutical kinetics, and in the use of those image data to identify the important source regions and

assign activity levels to them. To determine radiation dose, the counts seen in the images must be converted to absolute values of activity (Bq or mCi), which requires a known calibration factor for the camera, and collected data permit correction of the raw images for radiation attenuation and scatter. In planar imaging, the external conjugate view counting pair (anterior/posterior) as the most common method used to obtain quantitative data for dosimetry. In this method, the source activity A_j is given by the expression:

$$A_j = \sqrt{\frac{I_A I_P}{e^{-\mu_e t} C}} f_j \quad (10)$$

$$f_j = \frac{(\mu_j t_j / 2)}{\sinh(\mu_j t_j / 2)} \quad (11)$$

where I_A and I_P are the observed counts in the anterior and posterior projections (counts/time), t is the overall patient thickness, μ_e is the effective linear attenuation coefficient, C is system calibration factor C (count rate per unit activity), and the factor f represents a correction for the source region attenuation coefficient (μ_j) and source thickness (t_j) (i.e., source self-attenuation correction). This expression assumes that the views are perfectly collimated (i.e. they are oriented towards each other without offset) under the model of narrow beam geometry without significant scattered radiation effects. Corrections for scatter are usually necessary, and a number of methods have been proposed. One relatively straightforward correction procedure for scatter compensation involves establishing adjacent windows on either side of the photopeak window, with the area of the two similar adjacent windows equal to that of the photopeak. The corrected (true) photopeak counts C_T are given by the expression:

$$C_T = C_{pp} - F_S * (C_{LS} + C_{US}) \quad (12)$$

where C_{pp} is the total count recorded within the photopeak window, while C_{LS} and C_{US} are the counts within the lower and upper scatter windows, respectively. If the areas of the scatter windows are not equal (in sum) to that of the photopeak window, then an appropriate scaling factor (F_S) should be applied. Subtraction of the adjacent windows is assumed to compensate for the high-energy photon scatter tail upon which the true photopeak events are superimposed. Even if the areas of the scatter windows are equal to that of the photopeak window, use of a scaling factor other than unity may provide the best correction for scatter in a given system with a particular radionuclide. This may be determined by the study of a known volume source in a water phantom whose dimensions are similar to that of a human subject.

Other corrections are often required as well. Whenever a ROI is drawn over a source region on a projection image, some counts from the region will contain counts from activity in the subject's body that is outside of the identified source, scattered radiation from other ROIs, background radiation, and other sources. A background ROI is usually drawn over some region of

the body that is close to the source ROI and which, in the investigator's judgment, best represents the underlying and overlying tissues in which the source resides and which will provide the best estimate of a background count rate to be subtracted from the source ROI. Background ROIs should not be drawn over a major blood vessel or other body structure that contains a high level of activity, as this will remove too much background from the source ROI. The exact prescribing of locations and sizes of background ROIs is very difficult, and methods vary considerably between investigators. This can lead to markedly different results for the final estimates of activity assigned to a source ROI. This process should be carried out with caution and attention given to the above points for the best and most reproducible results. For quantification of counts in the total body, or in the check source placed externally to the body, a ROI should be drawn away from the subject's body, also away from any "star pattern" streaks that may accompany the source image, but close enough to capture a typical number of counts per pixel that represents background and scattered radiation within the imaging area close to the subject.

It is not uncommon for some organs or tumours to have overlapping regions on projection images. The right kidney and liver are frequently partially superimposed on such images, as are the left kidney and spleen, for example. When organ overlap occurs, an estimate of the total activity within a source can be obtained by a number of approximate methods. For paired organs, such as kidneys and lungs, one approach is to simply quantify the activity in one of the organs for which there is no overlap with other organs, and multiply the number of counts in this organ by two to obtain the total counts in both organs. Another approach is to draw a ROI over the organ region in scans where there is overlap, count the number of pixels and note the average count rate per pixel, then use a ROI from another image in which there is no apparent overlap and the whole organ is clearly visible; count the number of pixels in a larger ROI drawn on this image, and then multiply the count rate per pixel from the first image by the number of pixels in the second image. Or, equivalently, take the total number of counts in the first image and multiply by the ratio of the number of pixels in the second to the first image ROIs. If a significant overlap of images with another organ is not possible, an approximate ROI may need to be drawn just from the knowledge of the typical shapes of such organs. This kind of approximation is obviously not ideal, but may be necessary.

In addition, calibration coefficients for each radionuclide and gamma camera/collimator combination must be obtained by imaging a small source of known activity for a fixed amount of time. The attenuation characteristics of the camera may be studied by imaging this source with various known thicknesses of tissue-equivalent material interposed between the source and camera, and fitting the results (counts versus thickness) to an exponential function.

Quantification of tomographic data

Tomographic imaging offers the potential for improved dosimetric accuracy due to its increased contrast when compared with planar imaging. Tomographic data are particularly useful for dosimetry where there is suspected heterogeneous uptake of activity in the source organ or underlying or overlying background activity. To date, Positron Emission Tomography (PET) data have been little used for dosimetry, although PET quantification is an active area of research in its own right. Standardised uptake values (SUVs) are used to quantify radiotracer uptake (FDG) and, whilst prone to some uncertainty, are nevertheless used clinically with more regularity than quantification of Single Photon Emission Computed Tomography (SPECT) or planar data. SUVs are defined as

$$SUV = \frac{\text{tracer activity concentration in tissue}}{\text{injected tracer activity} / \text{patient weight}} \quad (13)$$

Quantification of SPECT data is accomplished in a number of steps:

1. **Data acquisition:** Data acquisition parameters include the number and timing of scans, as detailed above. With allowance made for adequate statistics and spatial resolution, no special criteria are required for the number of projections or matrix size, which are usually according to standard local protocols. However, it is worth noting that for many therapy scans, patients will have a relatively high level of activity so that camera sensitivity is not an issue. Data acquired soon after administration for example, may require scan times of only 5 seconds per view, so a full scan can be acquired in less than 10 minutes, which will not impact greatly on the daily routine of the nuclear medicine department. Collimators should be carefully chosen to suit the radionuclide being imaged.
2. **Deadtime corrections:** Scintillation cameras are designed for use with low levels of Tc-99m and so are poorly adapted for use with high activities of, for example, I-131. A common problem with these systems is that of deadtime, whereby the counts registered do not increase linearly with the activity in the field of view. Both paralyzable and non-paralyzable systems may be characterised for their deadtime behavior so that correction factors that can be directly applied to the image data may be obtained.
3. **Scatter correction:** Scatter correction methods are generally performed by the application of scatter windows placed adjacent to the photopeak. Frequently triple energy window (TEW) scatter correction is performed, as detailed above, although dual energy windows are also employed. A number of authors have explored the use of a large number of scatter windows [15] or the acquisition of list mode

data [16] although limitations are often imposed by the system used.

4. **Attenuation correction:** Attenuation correction is a crucial step in the quantification of emission data and a number of techniques have been used. The most basic method employed is that of Chang *et al* [17] who assume that the imaged volume is uniformly filled with water. More complex solutions, that to date have seldom been used in clinical practice, involve adaptation of a patient CT scan to provide an attenuation map [18].
5. **Reconstruction:** Image reconstruction can be divided into filtered back projection and iterative techniques, and can incorporate scatter and attenuation correction. Each of these techniques has a number of variables that may be employed, including smoothing parameters and the number of iterations. The effect on quantification of adjusting these parameters should be studied carefully on a case-specific basis.
6. **Quantification:** Conversion of counts to absolute values of activity may be performed in a number of ways. As specified above for the processing of planar data, it is possible to include a source of known activity within the field of view at the time of scanning. An approach used by some authors is to construct calibration phantoms that are aimed to emulate the patient. However, the ideal approach is to characterise the camera system so that conversion factors may be obtained without recourse to phantoms or external sources while taking into account patient CT data.

Quantification of image data has been considered for many years, although as yet there are no standardised methods for quantifying SPECT or PET data. This remains the largest single obstacle to accurate dosimetry, and is currently a strong focus of research [16, 19, 20]. It is probable that this task will be made easier with the advent of dual modality scanners and it is hoped that in time manufacturers will develop systems that are adapted to high energy high activity imaging, whereby camera sensitivity may be sacrificed to some extent in favour of spatial and energy resolution.

Absorbed Dose and the Biologically Effective Dose (BED)

The intermittent and sparse application of dosimetry for targeted radionuclide therapy (TRT), and the wide variation of methods employed, mean that to date few correlations between calculated absorbed doses and either therapeutic response or degree of toxicity have been seen. A further complication is caused by the fact that patients treated with TRT often present with disseminated disease, and after prior treatment with surgery, external beam radiotherapy and/or chemotherapy, are likely to respond differently to similar treatment with radionuclides. Consideration of

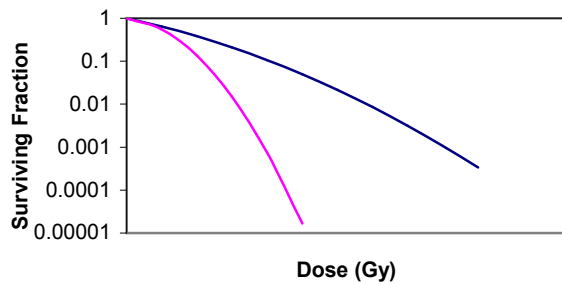


Figure 2 Cell survival curves as a function of the α/β ratio.

radiobiological principles is essential to enable treatment optimisation in external beam radiotherapy.

Radiobiological principles that apply to external beam radiotherapy may be applied to TRT with suitable modifications. Thus, the standard model of cell survival gives the fraction of cells surviving the irradiation (SF) as a function of the dose delivered (D):

$$\ln(SF) = -\alpha D - \beta D^2 \quad (14)$$

where α and β are disease- or even patient-specific parameters related to radiosensitivity, and the ratio of these parameters determine the shape of the cell survival curve (Figure 2). It is considered that α governs cell death from single hits, whilst β is dependent on the absorbed dose rate. It is therefore this term that is of greater importance in TRT [21]. A dose protraction factor, G, has been added to this model [22, 23] to accommodate the effect on cell kill by the change in absorbed dose rate, resulting in the more precise equation:

$$G = \frac{2}{D^2} \int_0^\infty \dot{D}(t) \int_0^t \dot{D}(t') e^{-\mu(t-t')} dt' dt \quad (15)$$

where μ is the constant of sub-lethal damage repair and t' is a time-point during the treatment prior to time t.

In practice, the large variation in absorbed dose rates for the radionuclides used in TRT mean that the application of this model is somewhat impractical. The Biologically Effective Dose (BED) was introduced to address these concerns [24, 25] and is defined as

$$BED = -\frac{\ln(SF)}{\alpha} \quad (16)$$

This model has been used to compare absorbed doses delivered with TRT, with those delivered with external beam radiotherapy using the following equations:

For external beam radiotherapy:

$$BED_{EBT} = D_{EBT} \left(1 + \frac{D_{EBT} / n}{\alpha / \beta} \right) \quad (17)$$

and for TRT:

$$BED_{TRT} = D_{TRT} \left(1 + \frac{D_{TRT} \lambda}{(\mu + \lambda)(\alpha / \beta)} \right) \quad (18)$$

As TRT is frequently used to treat patients with a wider variation in disease progression and treatment background, and because of the implications of the heterogeneity of uptake of a radionuclide [26], the application of radiobiological concepts are arguably of greater relevance than is the case for external beam radiotherapy, although this remains an area in need of significant research [27]. It is possible that radiobiological arguments may be employed to combine TRT and external beam radiotherapy [28].

STATUS OF DOSE CALCULATIONAL APPROACHES

Diagnostic agents

Dose calculations for diagnostic agents are developed using a combination of animal data and human subject (healthy volunteers or patients) during the drug approval process. Animal data may be extrapolated by a variety of methods, none of which is necessarily more correct than the other [29]. Human data are most often analysed using the conjugate-view approach described above, although for some positron emitting agents, positron emission tomography (PET) may be used to obtain quantitative data for dosimetry [30]. Dosimetry for these agents developed as typical values for average adults and children [31, 32] are usually accepted as adequate.

Therapeutic agents

Imaging of patients to obtain anatomical and physiological information has progressed substantially in the last decade. Anatomic information obtained from medical images, e.g. with MRI or CT, can be expressed in 3 dimensions (3D) in voxel format, with typical resolutions on the order of 1 mm. Similarly, SPECT and PET imaging systems can provide 3D representation of activity distributions within patients, with typical resolutions of around 5-10 mm. The newest systems now combine CT with both PET and SPECT state of the art imaging systems on the same imaging gantry, so that patient anatomy and tracer distribution can be imaged during a single imaging session without the need to move the patient, thus greatly improving and facilitating image registration. The use of Monte Carlo radiation transport codes with knowledge of patient anatomy will result in a significant improvement in the accuracy of dose calculations. Radiation dose calculations for nuclear medicine applications have been mostly relegated to abstract and theoretical calculations, used to establish dosimetry for new agents and provide reasonable dose estimates to support radiopharmaceutical package inserts and for use in open literature publications. When patients are treated in therapy with radiopharmaceuticals, careful, patient-specific optimisation is not performed, as is routine in radiation therapy with external sources of radiation i.e., radiation producing machines and brachytherapy. There are several reasons for this. One involves the limitations on spatial resolution and

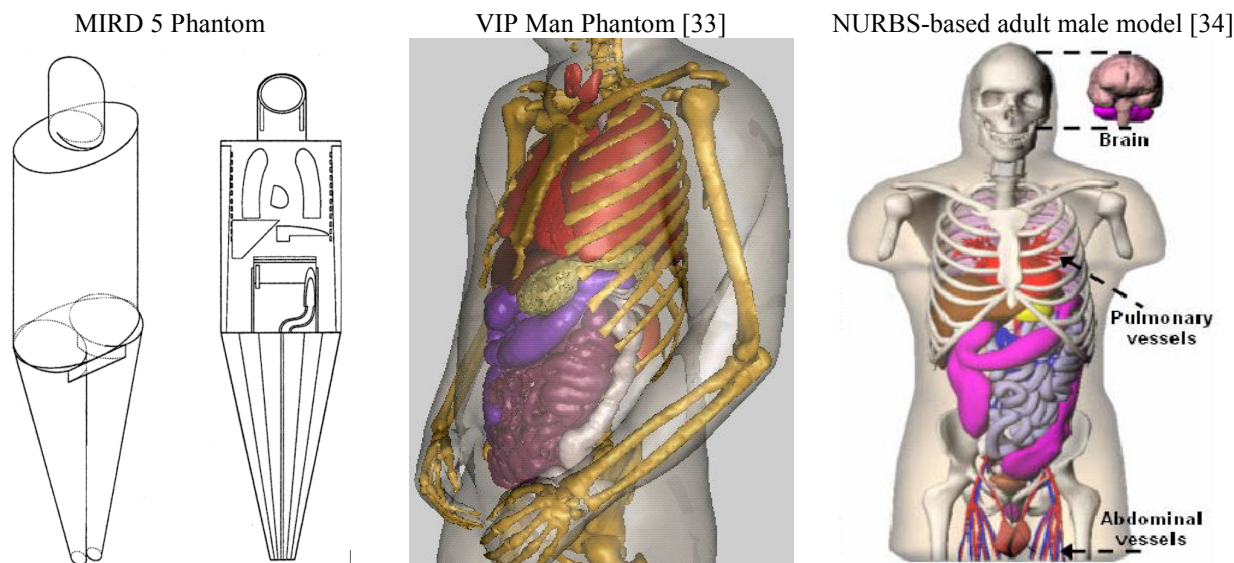


Figure 3 Comparison of the realism of the traditional MIRD body models with those being used to support current dose modelling efforts.

accuracy of activity quantification with nuclear medicine cameras. Another has to do with the realism and specificity to an individual patient of available body models. The models described above were designed to represent the “reference” adult male and female, children, and so on. Besides using geometric primitives to represent the body and its various organs, only one model is available for any category of individual, so dose estimates calculated using this approach will contain significant uncertainties when applied to any subject, and physicians understandably have low confidence in the use of these results to plan individual subject therapy. Thus, unfortunately for the patients, a “one dose fits all” approach to therapy is usually employed, with significant caution resulting in administration of lower than optimum levels of activity to the majority of subjects. The use of image-based models, not only to develop new “reference” phantoms, but also to permit the use of patient-specific models for each therapy patient, is now well-developed. Internal dosimetry is thus poised to truly enter a “Golden Age” in which it will become a more integral part of cancer care, as dosimetry is used in external source radiotherapy. The realism of the newer models is shown in Figure 3, with comparison to the form of the existing models developed and implemented in the historical MIRD system.

Image-based Computational Tools

Several efforts to use image data in dose calculations, as described above, include the 3D-ID code from the Memorial Sloan-Kettering Cancer Center [35], the SIMDOS code from the University of Lund [36], the RTDS code at the City of Hope Medical Center [37], the RMDP code from the Royal Marsden Hospital [38] and

the DOSE3D code [39]. The code with the most clinical experience to date is the 3D-ID code. These codes either rely on the standard geometrical phantoms (MABDose and DOSE3D) or patient-specific voxel phantom data (3DID and SIMDOS) and various in-house written routines to perform photon transport. Neither has a particularly robust and well-supported electron transport code, such as is available in EGS [40], MCNP [41], or GEANT [42]. The PEREGRINE code [43] has also been proposed for three-dimensional, computational dosimetry and treatment planning in radioimmunotherapy.

The usual approach used in these codes is to assume that electron energy is absorbed wherever the electron is first produced. The development and support of electron transport methods is quite complex, as evidenced by ongoing intensive efforts by both the EGS4 and MCNP computer code working groups. It is not reasonable to expect in-house written codes to deal effectively with electron transport. In areas of highly non-uniform activity distribution, such as an organ with multiple tumours with evidence of enhanced uptake of an antibody, explicit transport of both photons and electrons is needed to characterise dose distributions adequately.

CLINICAL EXPERIENCE WITH DOSIMETRY

Clinical applications of dosimetry to TRT have to date been limited to sporadic instances rather than comprehensive clinical trials. The lack of standardised methodology means that results are difficult to compare directly, although there is emerging evidence that dosimetry can prove to be of practical benefit in aiding the clinician to produce informed decisions. Although

dosimetry has been applied to a wide variety of diseases, there are a number of specific examples where it is likely to be of particular benefit.

Benign thyroid disease

There has been continual debate on the potential application of dosimetry to benign thyroid disease. Several authors have advocated that administered activities should be tailored to the individual patient to deliver a prescribed absorbed dose, although the majority of therapies are based on fixed activities. However, it has been shown that absolute uptake of radioiodine varies widely from patient to patient and is markedly more pronounced for autonomous nodules than for normal tissue [44]. The same authors also examined the use of I-124 NaI PET to perform tracer dosimetry and concluded that absorbed dose estimates could be made with an accuracy of within 10%. It has been shown that an absorbed therapeutic dose can be predicted by a prior tracer administration to within a degree of accuracy that would enable patient-specific treatment planning [45, 46]. It has been further shown that the rate of hypothyroidism resulting from the treatment of Graves' disease with radioiodine is correlated with the absorbed dose [47].

Thyroid Cancer

Treatment of thyroid cancer with ^{131}I NaI is the most common oncological application of TRT and has been used for nearly seven decades. There have been few changes in treatment regimens in that time, although there is no internationally agreed standard on how to perform treatment. In the majority of cases, treatments are based on fixed activities rather than absorbed doses, although there have been exceptions [48, 49]. Typically, patients will be given 1-3 GBq for ablation, and 3-20 GBq for a subsequent therapy [50]. Benua *et al.* [51] have administered according to a whole-body dose. Some authors have used ^{124}I NaI to perform dosimetry for the treatment of thyroid cancer [52, 53]. Where dosimetry has been performed, there is ample evidence that a wide range of tumour absorbed doses are delivered from fixed activities [53, 54]. It is probable that because of the relative simplicity of treatment, the lack of complications caused by other therapies, and its widespread use, radioiodine treatment of thyroid cancer offers the greatest potential for determining the dose-response criteria in a multi-centre setting that would lead to patient-specific treatment [55]. The issue of thyroid stunning would need to be circumvented although there is still doubt as to the level of diagnostic activity above which stunning occurs, whether the stunning phenomena is relevant for ^{123}I , ^{124}I , and indeed whether stunning is a real effect as such or whether it is an early therapeutic effect [56-58].

MIBG therapy for neuroendocrine tumours

I-131 meta-iodobenzylguanidine (mIBG) has been used for 20 years for the treatment of adult and paediatric neuroendocrine tumours, including pheochromocytoma,

paraganglioma and neuroblastoma. Administration protocols vary widely from standard administrations of 7.4 GBq to activities larger than 30 GBq for adults [59-61]. As with radioiodine treatment of thyroid cancer, the number and frequency of administrations also vary widely from centre to centre. Current problems with this therapy that could be addressed with dosimetry include the issue of carrier-added mIBG, since at present only a small fraction of the mIBG that is infused is labelled with I-131. Where dosimetry has been performed it has been shown that a wide variation in absorbed doses to either the whole-body or to the tumour or normal organs result from fixed administered activities [60, 62, 63]. A multi-centre dosimetry-led clinical trial aimed at relapsed or refractory neuroblastoma that recently commenced in Europe aims to administer a whole-body absorbed dose of 4 Gy in 2 fractions [61]. This and similar trials in the US are leading to the delivery of relatively high activities.

Radioimmunotherapy

The use of monoclonal antibodies for cancer treatment has been well established and is currently an area of clinical research that is rapidly increasing. The most common target for monoclonal antibody (mAB) therapy is lymphoma, with a number of centres having developed their own mAB's [64-66]. Two products, Bexxar and Zevalin have been approved by the US FDA for treatment of relapsed or refractory B-cell non-Hodgkin's lymphoma. Both use the anti-CD20 antibody although the major difference is that Bexxar employs ^{131}I as the radionuclide whereas Zevalin uses the longer range beta emitter ^{90}Y . The clinical efficacies of these treatments have yet to be directly compared in a trial. A key element of the treatment with Bexxar is that administration is based on a whole-body dose of 0.75 Gy [67], whereas for Zevalin, dosimetry was not recommended [68].

Peptide therapy

Peptide therapy for neuroendocrine tumours has recently emerged with the development of somatostatin analogues such as the compound DOTA-DPhe(1)-Tyr(3)-octreotide (DOTATOC). Although relatively few centers have performed this treatment, there have been a small number of dosimetric studies carried out [69]. Barone *et al.* [70] measured the kidney absorbed dose from administrations of 8.1 GBq-22.9 GBq of ^{90}Y DOTATOC, and after taking into account the biologically effective dose (BED), found a strong correlation between BED and creatinine clearance. A study by Hindorf *et al.* (in press) found that tumour absorbed doses resulting from a fixed administration of ^{90}Y DOTATOC varied widely on an inter-patient basis, although in repeated treatments the intra-patient variation was much smaller, indicating that it would be possible in principle to use dosimetric results from the first therapy to adjust subsequent therapies. Studies are ongoing to compare the relative efficacies of DOTATOC with DOTATATE and the optimal radionuclide [71].

Summary of Clinical Experience

The clinical introduction of internal dosimetry for TRT has been slow and is still far from being implemented routinely, despite a European directive stating that 'For all medical exposure of individuals for radiotherapeutic purposes, including nuclear medicine for therapeutic purposes, exposures of target volumes shall be individually planned; taking into account that doses of non-target volumes and tissues shall be as low as reasonably achievable and consistent with the intended radiotherapeutic purpose of the exposure' [72]. In cases where dosimetry is performed, the methodology employed is adapted from calculations derived for radiation protection rather than radiotherapy. Recent studies have shown conclusively that the administration of fixed activities results in a wide range of absorbed doses and there is now initial evidence to suggest that patient outcome is more likely to be correlated with absorbed dose rather than administered activity. It is likely that in the near future, internal dosimetry for both tumour and normal organs will become routine clinical practice, aided by improved techniques and possibly the application of radiobiological considerations. This will facilitate individualised treatment planning and the administration of cocktails of radionuclides.

THE CASE FOR OPTIMISATION

Physicians generally administer similar levels of activity or activity per unit total body mass to all patients [73]. This has been reasonably successful in the use of radioiodines against thyroid cancer and hyperthyroidism, as the "therapeutic window" (difference in dose levels between what is experienced by the tumour and that experienced by the most important normal tissue) is large. Nonetheless, some centres are now moving towards the use of patient-specific dose calculations even for iodine therapy, to optimise the therapeutic regime and to try to minimise the risk of unwanted side effects such as sialadenitis and sicca syndrome [74]. In other recently evolving forms of therapy, however, (e.g. the use of monoclonal antibodies and radiolabeled peptides in therapy), the tumour-to-normal tissue absorbed dose ratio may be low. Without the use of a patient-specific treatment planning strategy based on radiation absorbed dose, patients are frequently treated cautiously and given low amounts of the therapeutic agent, to avoid deleterious effects in normal tissues (most notably the bone marrow). Different patients will have different levels of tumour and normal tissue uptake concentrations, as well as in the clearance rates at which activity leaves these tissues. Patients who clear the activity more slowly from their bodies will necessarily receive higher doses to marrow and other normal tissues than those with faster rates of elimination. Thus, only some patients will receive optimal care, and a majority of patients will receive a lower than optimal administration of activity. This usually results in no deleterious effects in normal tissues, but suboptimal therapy being delivered to the

malignant tissues, with poor response rates and high rates of relapse. As was stated by Siegel *et al.* [75]:

"If one were to approach the radiation oncologist or medical physicist in an external beam therapy program and suggest that all patients with a certain type of cancer should receive the exact same protocol (beam type, energy, beam exposure time, geometry, etc.), the idea would certainly be rejected as not being in the best interests of the patient. Instead, a patient-specific treatment plan would be implemented in which treatment times are varied to deliver the same radiation dose to all patients. Patient-specific calculations of doses delivered to tumours and normal tissues have been routine in external beam radiotherapy and brachytherapy for decades. The routine use of a fixed GBq/kg, GBq/m², or simply GBq, administration of radionuclides for therapy is equivalent to treating all patients in external beam radiotherapy with the same protocol. Varying the treatment time to result in equal absorbed dose for external beam radiotherapy is equivalent to accounting for the known variation in patients' uptake and retention half-time of activity of radionuclides to achieve equal tumour absorbed dose for internal-emitter radiotherapy. It has been suggested that fixed activity-administration protocol designs provide little useful information about the variability among patients relative to the normal organ dose than can be tolerated without dose-limiting toxicity compared to radiation dose-driven protocols."

Thierens *et al.* [76] noted that "...patient-specific dose calculations in radionuclide therapy are difficult to perform and possibly subject to large error. Therefore, individual dosimetry-based activity calculations are not routinely applied yet and a large variety of methodologies exists for determining the administered activity in clinical practice..." They also noted, however, that "...as absorbed dose estimates become more patient-specific, an improved correlation between the administered activity and the clinical outcome may be expected. It is clear that a patient-specific treatment planning will improve the quality of radionuclide therapy substantially, especially in a curative setting."

Treating all nuclear medicine patients with a single, uniform method of activity administration amounts to consciously choosing a lower standard of care than patients who receive radiation externally for cancer treatments. Some have insisted that hypothesis-driven testing proves statistically that nuclear medicine therapy patients treated with consideration of individual dosimetry have better and more durable outcomes than those treated under the current practice of administering the same activity levels to all patients, as a prerequisite to considering dosimetry as routine practice. This sets a very high hurdle for the inclusion of this practice, and certainly puts it off many years into the future. In the meantime, tens of thousands of patients will be receiving suboptimal therapy, and no widespread data gathering will occur to improve dosimetry methods and understanding of the relationship between doses received and outcomes observed. We take it as given that

response to radiation will correlate with absorbed dose more closely than it will with administered activity, or the intention to treat. It is essential that in all forms of radiotherapy with internal emitters, a patient-individualised dose calculation be made when possible for the most important tumours for which a specific uptake of the radiopharmaceutical can be derived, and for the most important normal tissue at risk (generally the bone marrow, but possibly the lungs, kidneys, or other organs). This is needed not only to provide a better quality of therapy to patients treated currently, but also to establish a database of literature that can be used to understand the variability between subjects and the range of uptake and clearance values to be expected for different therapy agents. Standardised methods for calculating dose are well established and automated at present, and should be used to provide dose calculations that are comparable and reproducible between institutions.

REFERENCES

- Snyder WS, Fisher HL Jr, Ford MR *et al.* Estimates of absorbed fractions for monoenergetic photon sources uniformly distributed in various organs of a heterogeneous phantom. *J Nucl Med* 1969; Suppl 3:7-52.
- International Commission on Radiological Protection. Task Group Report on Reference Man. Oxford: Pergamon Press, 1975. (ICRP Publication; 23).
- International Commission on Radiological Protection. Basic Anatomical and Physiological Data for Use in Radiological Protection: Reference Values. Elsevier Health, 2003. (ICRP Publication; 89).
- Snyder W, Ford M, Warner G. Estimates of specific absorbed fractions for photon sources uniformly distributed in various organs of a heterogeneous phantom. New York: Society of Nuclear Medicine, 1978. (MIRD Pamphlet; 5).
- Snyder W, Ford M, Warner G *et al.* A tabulation of dose equivalent per microcurie-day for source and target organs of an adult for various radionuclides. Oak Ridge National Laboratory, 1975; ORNL-5000.
- Cristy M, Eckerman K. Specific absorbed fractions of energy at various ages from internal photons sources. Oak Ridge, TN: Oak Ridge National Laboratory, 1987; ORNL/TM-8381 V1-V7.
- Stabin MG. MIRDOSE: personal computer software for internal dose assessment in nuclear medicine. *J Nucl Med* 1996; 37(3):538-46.
- Stabin M, Watson E, Cristy M *et al.* Mathematical models and specific absorbed fractions of photon energy in the nonpregnant adult female and at the end of each trimester of pregnancy. 1995; ORNL/TM-12907.
- Spiers FW. Beta dosimetry in trabecular bone. Mays CW, ed. *Delayed Effects of Bone-Seeking Radionuclides*. Salt Lake City, UT: Univ of Utah Press, 1969: 95-108.
- Eckerman KF, Stabin MG. Electron absorbed fractions and dose conversion factors for marrow and bone by skeletal regions. *Health Phys* 2000; 78(2):199-214.
- Bouchet LG, Bolch WE, Howell RW *et al.* S values for radionuclides localized within the skeleton. *J Nucl Med* 2000; 41(1):189-212.
- Stabin MG, Eckerman KF, Bolch WE *et al.* Evolution and status of bone and marrow dose models. *Cancer Biother Radiopharm* 2002; 17(4):427-33.
- Stabin MG, Sparks RB, Crowe E. OLINDA/EXM: the second-generation personal computer software for internal dose assessment in nuclear medicine. *J Nucl Med* 2005; 46(6):1023-7.
- Siegel JA, Thomas SR, Stubbs JB *et al.* MIRD pamphlet no. 16: Techniques for quantitative radiopharmaceutical biodistribution data acquisition and analysis for use in human radiation dose estimates. *J Nucl Med* 1999; 40(2):37S-61S.
- Buvat I, Rodriguez-Villafuerte M, Todd-Pokropek A *et al.* Comparative assessment of nine scatter correction methods based on spectral analysis using Monte Carlo simulations. *J Nucl Med* 1995; 36(8):1476-88.
- Guy MJ, Castellano-Smith IA, Flower MA. DETECT - Dual energy transmission estimation CT - for improved attenuation correction in SPECT and PET. *IEEE Trans Nucl Sci* 1998; 45:1261-7.
- Chang LT. A method for attenuation correction in radionuclide computed tomography. *IEEE Trans Nucl Sci* 1978; 25:638-43.
- Fleming JS. A technique for using CT images in attenuation correction and quantification in SPECT. *Nucl Med Commun* 1989; 10(2):83-97.
- Autret D, Bitar A, Ferrer L *et al.* Monte Carlo modeling of gamma cameras for I-131 imaging in targeted radiotherapy. *Cancer Biother Radiopharm* 2005; 20(1):77-84.
- Dewaraja YK, Wilderman SJ, Ljungberg M *et al.* Accurate dosimetry in I-131 radionuclide therapy using patient-specific, 3-dimensional methods for SPECT reconstruction and absorbed dose calculation. *J Nucl Med* 2005; 46(5):840-9.
- Dale RG. The application of the linear-quadratic dose-effect equation to fractionated and protracted radiotherapy. *Br J Radiol* 1985; 58(690):515-28.
- Sachs RK, Hahnfeld P, Brenner DJ. The link between low-LET dose-response relations and the underlying kinetics of damage production/repair/misrepair. *Int J Radiat Biol* 1997; 72(4):351-74.
- Lea DE, Catcheside DG. The Mechanism of the Induction by Radiation of Chromosome Abberations in *Tradescantia*. *J Genet* 1942; 44:216-45.
- Barendsen GW. Dose fractionation, dose rate and iso-effect relationships for normal tissue responses. *Int J Radiat Oncol Biol Phys* 1982; 8(11):1981-97.
- Fowler JF. The linear-quadratic formula and progress in fractionated radiotherapy. *Br J Radiol* 1989; 62(740):679-94.
- Malaroda A, Flux GD, Buffa FM *et al.* Multicellular dosimetry in voxel geometry for targeted radionuclide therapy. *Cancer Biother Radiopharm* 2003; 18(3):451-61.
- O'Donoghue JA, Sgouros G, Divgi CR *et al.* Single-dose versus fractionated radioimmunotherapy: model comparisons for uniform tumor dosimetry. *J Nucl Med* 2000; 41(3):538-47.
- Bodey RK, Evans PM, Flux GD. Application of the linear-quadratic model to combined modality radiotherapy. *Int J Radiat Oncol Biol Phys* 2004; 59(1):228-41.
- Blau M. Letter: Radiation dosimetry of I-131-iodocholesterol: The pitfalls of using tissue concentration data. *J Nucl Med* 1975; 16(3):247-9.
- Sgouros G, Kolbert KS, Sheikh A *et al.* Patient-specific dosimetry for I-131 thyroid cancer therapy using I-124I PET and 3-dimensional-internal dosimetry (3D-ID) software. *J Nucl Med* 2004; 45(8):1366-72.
- International Commission on Radiological Protection. *Radiation Dose to Patients from Radiopharmaceuticals*. New York: Pergamon, 1989. (ICRP Publication; 53).
- International Commission on Radiological Protection. *Radiation Dose To Patients From Radiopharmaceuticals*. New York: Pergamon, 2000. (ICRP Publication; 80).
- Xu XG, Chao TC, Bozkurt A. VIP-Man: an image-based whole-body adult male model constructed from color photographs of the Visible Human Project for multi-particle Monte Carlo calculations. *Health Phys* 2000; 78(5):476-86.
- Segars JP. Development and Application of the New Dynamic NURBS-based Cardiac-Torso (NCAT) Phantom [Ph.D. Dissertation]. The University of North Carolina, 2001.
- Kolbert KS, Sgouros G, Scott AM *et al.* Implementation and evaluation of patient-specific three-dimensional internal dosimetry. *J Nucl Med* 1997; 38(2):301-8.
- Dewaraja YK, Wilderman SJ, Ljungberg M *et al.* Accurate dosimetry in I-131 radionuclide therapy using patient-specific, 3-dimensional methods for SPECT reconstruction and absorbed dose calculation. *J Nucl Med* 2005; 46(5):840-9.
- Liu A, Williams LE, Lopatin G *et al.* A radionuclide therapy treatment planning and dose estimation system. *J Nucl Med* 1999; 40(7):1151-3.

38. Guy MJ, Flux GD, Papavasileiou P *et al.* RMDP: a dedicated package for 131I SPECT quantification, registration and patient-specific dosimetry. *Cancer Biother Radiopharm* 2003; 18(1):61-9.
39. Clairand I, Ricard M, Gouriou J *et al.* DOSE3D: EGS4 Monte Carlo code-based software for internal radionuclide dosimetry. *J Nucl Med* 1999; 40(9):1517-23.
40. Bielajew A, Rogers D. PRESTA: the parameter reduced electron-step transport algorithm for electron Monte Carlo transport. *Nucl Instrum Methods* 1987; B18:165-81.
41. Briesmeister JF, ed. MCNP - A General Monte Carlo N-Particle Transport Code, Version 4C. Los Alamos National Laboratory, 2000; LA-13709-M.
42. Allison J *et al.* Geant4 Developments and Applications. *IEEE Trans Nucl Sci* 2006; 53:270-8.
43. Lehmann J, Hartmann Siantar C, Wessol DE *et al.* Monte Carlo treatment planning for molecular targeted radiotherapy within the MINERVA system. *Phys Med Biol* 2005; 50(5):947-58.
44. Eschmann SM, Reischl G, Bilger K *et al.* Evaluation of dosimetry of radioiodine therapy in benign and malignant thyroid disorders by means of iodine-124 and PET. *Eur J Nucl Med Mol Imaging* 2002; 29(6):760-7.
45. Canzi C, Zito F, Voltini F *et al.* Verification of the agreement of two dosimetric methods with radioiodine therapy in hyperthyroid patients. *Med Phys* 2006; 33(8):2860-7.
46. Carlier T, Salaun PY, Cavarec MB *et al.* Optimized radioiodine therapy for Graves' disease: two MIRD-based models for the computation of patient-specific therapeutic 131I activity. *Nucl Med Commun* 2006; 27(7):559-66.
47. Grosso M, Traino A, Boni G *et al.* Comparison of different thyroid committed doses in radioiodine therapy for Graves' hyperthyroidism. *Cancer Biother Radiopharm* 2005; 20(2):218-23.
48. Furhang EE, Larson SM, Buranapong P *et al.* Thyroid cancer dosimetry using clearance fitting. *J Nucl Med* 1999; 40(1):131-6.
49. Maxon HR, Thomas SR, Samaratunga RC. Dosimetric considerations in the radioiodine treatment of macrometastases and micrometastases from differentiated thyroid cancer. *Thyroid* 1997; 7(2):183-7.
50. Reiners C. Radioiodine therapy of thyroid cancer. *Tumordiagnostik & Therapie* 1998; 19:70-3.
51. Benua RS, Cicale NR, Sonenberg M *et al.* The relation of radioiodine dosimetry to results and complications in the treatment of metastatic thyroid cancer. *Am J Roentgenol Radium Ther Nucl Med* 1962; 87:171-82.
52. Ott RJ, Tait D, Flower MA *et al.* Treatment planning for 131I-MIBG radiotherapy of neural crest tumours using 124I-MIBG positron emission tomography. *Br J Radiol* 1992; 65(777):787-91.
53. Sgouros G, Kolbert KS, Sheikh A *et al.* Patient-specific dosimetry for 131I thyroid cancer therapy using 124I PET and 3-dimensional-internal dosimetry (3D-ID) software. *J Nucl Med* 2004; 45(8):1366-72.
54. Dorn R, Kopp J, Vogt H *et al.* Dosimetry-guided radioactive iodine treatment in patients with metastatic differentiated thyroid cancer: largest safe dose using a risk-adapted approach. *J Nucl Med* 2003; 44(3):451-6.
55. Hanscheid H, Lassmann M, Luster M *et al.* Iodine biokinetics and dosimetry in radioiodine therapy of thyroid cancer: procedures and results of a prospective international controlled study of ablation after rhTSH or hormone withdrawal. *J Nucl Med* 2006; 47(4):648-54.
56. Lassmann M, Luster M, Hanscheid H *et al.* Impact of 131I diagnostic activities on the biokinetics of thyroid remnants. *J Nucl Med* 2004; 45(4):619-25.
57. Sisson JC, Avram AM, Lawson SA *et al.* The so-called stunning of thyroid tissue. *J Nucl Med* 2006; 47(9):1406-12.
58. Woolfenden JM. Thyroid stunning revisited. *J Nucl Med* 2006; 47(9):1403-5.
59. Hoefnagel CA. Nuclear medicine therapy of neuroblastoma. *Q J Nucl Med* 1999; 43(4):336-43.
60. Matthay KK, Panina C, Huberty J *et al.* Correlation of tumor and whole-body dosimetry with tumor response and toxicity in refractory neuroblastoma treated with (131I)-MIBG. *J Nucl Med* 2001; 42(11):1713-21.
61. Gaze MN, Chang YC, Flux GD *et al.* Feasibility of dosimetry-based high-dose 131I-meta-iodobenzylguanidine with topotecan as a radiosensitizer in children with metastatic neuroblastoma. *Cancer Biother Radiopharm* 2005; 20(2):195-9.
62. Monsieurs M, Brans B, Bacher K *et al.* Patient dosimetry for 131I-MIBG therapy for neuroendocrine tumours based on 123I-MIBG scans. *Eur J Nucl Med Mol Imaging* 2002; 29(12):1581-7.
63. Flux GD, Guy MJ, Papavasileiou P *et al.* Absorbed dose ratios for repeated therapy of neuroblastoma with I-131 mIBG. *Cancer Biother Radiopharm* 2003; 18(1):81-7.
64. DeNardo GL, DeNardo SJ, Shen S *et al.* Factors affecting 131I-Lym-1 pharmacokinetics and radiation dosimetry in patients with non-Hodgkin's lymphoma and chronic lymphocytic leukemia. *J Nucl Med* 1999; 40(8):1317-26.
65. Linden O, Tennvall J, Cavallin-Stahl E *et al.* Radioimmunotherapy using 131I-labeled anti-CD22 monoclonal antibody (LL2) in patients with previously treated B-cell lymphomas. *Clin Cancer Res* 1999; 5(10 Suppl):3287s-91s.
66. Chatal JF, Faivre-Chauvet A, Bardies M *et al.* Bifunctional antibodies for radioimmunotherapy. *Hybridoma* 1995; 14(2):125-8.
67. Wahl RL, Kroll S, Zasadny KR. Patient-specific whole-body dosimetry: principles and a simplified method for clinical implementation. *J Nucl Med* 1998; 39(8 Suppl):14S-20S.
68. Wiseman GA, White CA, Sparks RB *et al.* Biodistribution and dosimetry results from a phase III prospectively randomized controlled trial of Zevalin radioimmunotherapy for low-grade, follicular, or transformed B-cell non-Hodgkin's lymphoma. *Crit Rev Oncol Hematol* 2001; 39(1-2):181-94.
69. Cremonesi M, Ferrari M, Chinol M *et al.* Dosimetry in radionuclide therapies with 90Y-conjugates: the IEO experience. *Q J Nucl Med* 2000; 44(4):325-32.
70. Barone R, Walrand S, Valkema R *et al.* Correlation between acute red marrow (RM) toxicity and RM exposure during Y-90-SMT487 therapy. *J Nucl Med* 2002; 43:1267.
71. Esser JP, Krenning EP, Teunissen JJ *et al.* Comparison of [(177)Lu-DOTA(0),Tyr(3)]octreotate and [(177)Lu-DOTA(0),Tyr(3)]octreotide: which peptide is preferable for PRRT? *Eur J Nucl Med Mol Imaging* 2006; 33(11):1346-51.
72. EURATOM. Health protection of individuals against the dangers of ionising radiation in relation to medical exposure: Council directive 97/43. EURATOM, 1997.
73. Parthasarathy KL, Crawford ES. Treatment of thyroid carcinoma: emphasis on high-dose 131I outpatient therapy. *J Nucl Med Technol* 2002; 30(4):165-71; quiz 172-3.
74. Solans R, Bosch JA, Galofre P *et al.* Salivary and lacrimal gland dysfunction (sicca syndrome) after radioiodine therapy. *J Nucl Med* 2001; 42(5):738-43.
75. Siegel JA, Stabin MG, Brill AB. The importance of patient-specific radiation dose calculations for the administration of radionuclides in therapy. *Cell Mol Biol (Noisy-Le-Grand)* 2002; 48(5):451-9.
76. Thierens HM, Monsieurs MA, Bacher K. Patient dosimetry in radionuclide therapy: the whys and the wherefores. *Nucl Med Commun* 2005; 26(7):593-9.